Time-resolved x-ray diffraction and calorimetric studies at low scan rates

I. Fully hydrated dipalmitoylphosphatidylcholine (DPPC) and DPPC/water/ethanol phases

Boris G. Tenchov, Haruhiko Yao, and Ichiro Hatta

Department of Applied Physics, School of Engineering, Nagoya University, Chikusa-ku, Nagoya 464-01, Japan

ABSTRACT The phase transitions in fully hydrated dipalmitoylphosphatidylcholine (DPPC) and DPPC/water/ethanol phases have been studied by low-angle time-resolved x-ray diffraction under conditions similar to those employed in calorimetry (scan rates 0.05–0.5°C/min and uniform temperature throughout the samples). This approach provides more adequate characterization of the equilibrium transition pathways and allows for close correlations between structural and thermodynamic data. No coexistence of the rippled gel ($P_{\beta'}$) and liquid-crystalline (L_α) phases was found in the main transition of DPPC; rather, a loss of correlation in the lamellar structure, observed as broadening of the lamellar reflections, takes place in a narrow temperature range of ~100 mK at the transition midpoint. Formation of a long-living metastable phase, denoted by $P_{\beta'}$(mst), differing from the initial $P_{\beta'}$ was observed in cooling direction by both x-ray diffraction and calorimetry. No direct conversion of $P_{\beta'}$(mst) into $P_{\beta'}$ occurs for over 24 h but only by way of the phase sequence $P_{\beta'}$(mst) → $L_{\beta'}$ → $P_{\beta'}$. According to differential scanning calorimetry (DSC), the enthalpy of the $P_{\beta'}$(mst)-L_α transition is by ~5% lower than that of the $P_{\beta'}$-L_α transition. The effects of ethanol (Rowe, E. S. 1983. Biochemistry. 22:3299–3305; Simon, S. A., and T. J. McIntosh. 1984. Biochim. Biophys. Acta 773:169–172) on the mechanism and reversibility of the DPPC main transition were clearly visualized. At ethanol concentrations inducing formation of interdigitated gel phase, the main transition proceeds through a coexistence of the initial and final phases over a finite temperature range. During the subtransition in DPPC recorded at scan rate 0.3°C/min, a smooth monotonic increase of the lamellar spacing from its subgel (L_c) to its gel ($L_{\beta'}$) phase value takes place. The width of the lamellar reflections remains unchanged during this transformation. This provides grounds to propose a "sequential" relaxation mechanism for the subgel-gel transition which is not accompanied by growth of domains of the final phase within the initial one.

INTRODUCTION

Due to the high intensity of synchrotron x-rays, their application in diffraction studies of lipid-water phases results in a substantial reduction of exposure times and accumulation of stable diffraction patterns in <1 s. In comparison with conventional x-ray sources the time resolution is improved by some three to four orders of magnitude, and it becomes possible to observe in real time changes in diffraction patterns during various phase transitions taking place in these systems with temperature (1–9). With respect to temperature control, a common feature of these studies is that the diffraction data characterizing the phase transitions have been recorded during temperature jumps of at least several degrees centigrade per second (1–7), or during relatively fast heating and cooling scans of 5–10°C/min (8, 9). It is conceivable, however, that such temperature variations would be faster than the response times of the structural rearrangements and the investigated systems would be driven far away from their equilibrium states in the transition region. Another possible consequence of the fast temperature variations could be an appearance of relatively large temperature gradients within the sample volume from which diffraction data are collected. Such gradients might provoke an apparent coexistence of diffraction patterns which actually correspond to different temperatures. It is therefore desirable to perform time-resolved diffraction measurements during quasistatic temperature scans, i.e., in conditions similar to those currently employed in calorimetry: (a) low heating and cooling rates; (b) absence of temperature gradients within the sample. Undoubtedly, such measurements would provide more adequate characterization of lipid phase transitions and permit also to establish close correlations between structural and thermodynamic data.

In this work we made time-resolved low-angle x-ray diffraction measurements using precise temperature control. In a first application to lipid phase transitions, this approach was used to examine well-known systems: fully hydrated dipalmitoylphosphatidylcholine (DPPC) (11–17) and DPPC/water/ethanol phases (18–20). Complemented with data obtained by DSC and high-resolution temperature oscillation calorimetry, so called AC calorimetry, these measurements revealed previously unre-

---

B. G. Tenchov's permanent address is the Central Laboratory of Biophysics, Bulgarian Academy of Sciences, 1113 Sofia, Bulgaria.

ported features of the DPPC phase behavior and visualized distinct changes in the main transition mechanism induced by addition of ethanol. These results demonstrate the potential of the method in structural studies of phase transitions.

MATERIALS AND METHODS

Sample preparation

DPPC (1,2-dipalmitoyl-sn-glycero-3-phosphorylcholine) from three different sources (Avanti Polar Lipids, Inc., Birmingham, AL, chloroform solution; Fluka AG, Buchs, Switzerland, powder; Sigma Chemical Co., St. Louis, MO, powder) was used. No chromatographic tests for purity were performed, however, the narrow main transition recorded by calorimetry (<0.2°C) provides a sound guarantee that the lipid purity was similar to that in other studies and comparable with the claimed value of at least 99%. Actually, the main transition width of DPPC from Sigma Chemical Co. was consistently greater compared with DPPC from the other two sources. For this reason the lipid source is indicated everywhere in the figure legends. The DPPC chloroform solution (Avanti Polar Lipids, Inc.) was dried under vacuum for >20 h until constant weight was obtained. Multilamellar lipid vesicles were prepared by dispersing DPPC in required amounts of bidistilled deionized water (pH 5.3, conductivity <2 μS). The sealed dispersions were hydrated at 60°C for at least 1 h and vortexed several times at this temperature for 1–2 min. The lipid concentrations were 0.05 wt% in DSC, 10 wt% in AC calorimetry, and 20–25 wt% in the x-ray measurements. DPPC/water/ethanol samples were prepared by the same procedure using water/ethanol mixtures instead of pure water. The dispersions were usually stored at 4°C for several days before the measurements. The procedure used for sample preparation and storage was sufficient to ensure reproducible phase behavior of the lipid in identical successive heating-cooling cycles.

X-Ray diffraction

X-Ray experiments were carried out using a monochromatic (0.150 nm) and horizontally focused x-ray beam at station 15A of the Photon Factory (21). The cross-section of the beam as measured by Nitto Radocolor x-ray–sensitive films attached to the sample holder was rectangular with dimensions 1.6 × 0.7 mm (width × height). The incident photon flux was concurrently monitored by an ion chamber situated in front of the sample holder. Its intensity was typically in the range $(2 - 4) \times 10^8$ photons/s and was practically constant during particular temperature scans. The flux was reduced ~30 times by a glass slide and a 2 mm water layer in the sample holder (Fig. 1 B) and the estimated flux on the sample was ~10^7 photons/s.

Diffraction patterns were recorded using a one-dimensional position-sensitive proportional counter with 512 channels (PSPC, Rigaku, Tokyo, Japan) linked to the station computer. The PSPC was positioned vertically with the stopped main beam aiming at its center. In this way, two symmetric profiles were concurrently recorded each containing the lamellar first- and second-order reflections. The PSPC length used was 170 mm (462 channels). The sample-to-detector distance was 1,226 mm and the maximum angle was ~4°. The channel-to-channel distance of the PSPC was 0.368 mm and the angular resolution was 0.017°, equivalent to a resolution of 0.07–0.09 nm for spacings in the range 6–7 nm.

The sample holder consisted of an outer brass jacket and an inner aluminum cell with mylar windows (Fig. 1). The sample volume was 1 × 5 × 4 mm³ (thickness × width × height). The temperature was scanned or kept constant by circulating water between the jacket and
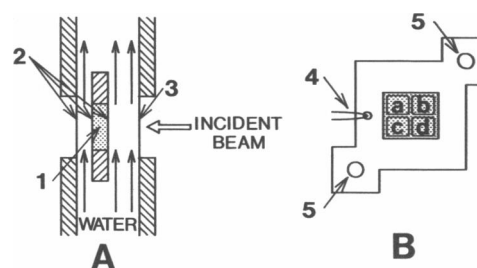

FIGURE 1 Sketch of the sample holder: (A) cross-section of outer jacket and inner cell; (B) inner cell cross-section perpendicular to the incident beam; (1) sample; (2) mylar windows; (3) glass window; (4) thermocouple; (5) holes for attachment screws. Four nonoverlapping sample parts from which diffraction data have been recorded are denoted by a–d.

the sample cell from a computer-controled water bath (RCS-20D, Messgeräte-werk Lauda, Dr. R. Wobser KG, Lauda-Königshofen, FRG). Temperature gradients within the sample were eliminated by using a holder in which water circulated also between the jacket and sample cell windows for the diffracted and incident x-rays (Fig. 1 A). The thicknesses of these water layers were 1 and 2 mm, respectively. The water flow was 13 liters/min. Because the inner cell was totally immersed into water and its only direct thermal contact with the outer jacket was through two relatively distant attachment screws (Fig. 1 B) we assume that the gradients within the sample were of the order of the temperature fluctuations. X-Ray measurements described under Experimental Results are consistent with this assumption.

The sample temperature was monitored using a chromel-alumel thermocouple planted into the inner cell (Fig. 1 B). Its readings were Perfectly linear heating and cooling scans were made by means of a computer control of the water bath setting voltage. The scan rate could be varied in the range 0–0.5°C/min. According to the water bath specification, its temperature stability is better than 0.020°C. This was consistent with the records of the sample temperature. The temperature fluctuations in the sample did not exceed 0.010°C at any fixed temperature (constant setting voltage of the bath) or during temperature scans.

The sample holder was mounted on a stage which could be translated vertically and horizontally with a precision of 0.01 mm by a servomotor with remote control. It was thus possible to change the sample position with respect to the incident beam in the course of the measurement and to record and compare diffraction patterns from at least four nonoverlapping parts of the sample, as shown in Fig. 1 B. This option was used to check temperature uniformity within the sample and detect possible radiation damage by comparing diffraction patterns of irradiated and nonirradiated portions of the lipid.

An accumulation time of 30 s was used for the individual diffraction patterns with a dead time of <1 ms between successive frames. Only raw data were used and no smoothing procedures were applied. The diffraction patterns were graphically represented by connecting intensities in neighboring channels with segments and for this reason they appear as segmental rather than smooth curves. Lamellar spacings were determined as a position of the channel with maximum intensity. The maximum error introduced by such a method cannot exceed one half of the distance between neighboring channels.

High-sensitivity DSC (HSDSC)

HSDSC measurements were made using a Privalov DASM-1M microcalorimeter (Special Bureau of Biological Instrumentation of the Acad-

emy of Sciences of the USSR, Moscow) (22) at heating rate 0.5°C/min. The cooling rate between two successive heating scans is not controllable in a DASM-1M calorimeter. It follows an approximately exponential law.

AC calorimetry

The design of the AC microcalorimeter and the measurement method used are described in detail elsewhere (23, 24). The temperature oscillation T_{ac} was varied between 1 and 10 mK, which ruled the temperature resolution. The oscillation frequency was 1 Hz. The resolution in T_{ac} is better than 0.1 mK. The quantity measured was the so-called dynamic heat capacity, defined in the present case as $C_p(1 \text{ Hz}) = Q_o/2\omega T_{ac}$, where Q_o is the amount of heat periodically supplied to the sample as to ensure a modulation of its temperature with an angular frequency ω. During lipid phase transitions the excess values of $C_p(1 \text{ Hz})$ are usually several times smaller than the corresponding values of the static excess C_p recorded by DSC. Respectively, the peak areas (enthalpy of the transitions) are also several times smaller. This difference is qualitatively understood as follows. The dynamic heat capacity reflects only heat absorbed in fast enough structural rearrangements accomplished within one cycle of temperature modulation (1 s in the present measurements), whereas heat absorbed by slow modes with longer response times does not contribute to its value.

With the present experimental arrangement it was possible to measure $C_p(1 \text{ Hz})$ during slow heating and cooling runs and to monitor also its evolution for a long time at constant temperature. In spite of the difficulties encountered in microscopic interpretations of the dynamic heat capacity, such measurements provide specific and rather sensitive characterization of the dynamics and reversibility of the lipid phase transitions which can be usefully compared with the diffraction data.

EXPERIMENTAL RESULTS

Time-resolved x-ray diffraction

Usually a scan rate of 0.5°C/min was initially used for an overview and to determine the phase transition boundaries. After that the same measurement was repeated with a fresh sample at 0.1°C/min. With an accumulation time of 30 s, the temperature resolution of the diffraction frames was 0.25 and 0.050°C at these two scan rates. The results at the two scan rates are in general agreement. Further we consider mainly the data of higher temperature resolution recorded at 0.1°C/min and do not analyze the scan rate dependence. A few experiments were made at scan rate 0.05°C/min. The subtransition was recorded at 0.3°C/min. Up to 55 successive frames were recorded in each temperature scan.

In these conditions the maximum exposure time of a lipid sample to the incident x-ray beam was closely below 30 min. It is known from a previous study (25) that exposures of this length to synchrotron x-rays can result in extensive radiation damage of DPPC which is not only detectable by chromatography but also displayed in marked changes of the diffraction patterns and visual appearance of the samples. Two types of experiments were made to check for such effects. First, by shifting the

samples with respect to the beam, we compared patterns from one irradiated for 30 min and three nonirradiated portions of the samples (Fig. 1 B). Measurements of this type were carried out with DPPC and dipalmitoylphosphatidylethanolamine (DPPE) at various temperatures, including those near the transition midpoints, where it might be expected that the diffraction patterns would be more sensitive to the presence of degradation products. Second, we compared identical temperature scans of fresh samples and samples already irradiated during a previous heating or cooling scan. Both types of experiments did not reveal differences between the x-ray patterns of the fresh and irradiated samples. We conclude therefore that in our conditions irradiation of up to 30 min (at least one heating or cooling scan) did not affect the lipid structures and phase behavior in a way detectable by low-angle x-ray diffraction. This is obvious from the scans shown in Figs. 2, 3, 5–8. Because radiation damage has been observed after much shorter exposures of ~5 min (25) we assume that the absence of noticeable radiation effects in our experiments is a consequence of a substantially lower incident beam intensity. Actually, the (wiggler-enhanced) flux intensity at the sample reported in reference 25 is ~200 times higher than that in the present work. It should be noted, however, that the lack of radiation effects in the diffraction patterns by no means rules out the existence of lipid degradation products and the possibility of their detection by more sensitive methods.

The temperature uniformity throughout the samples was checked by recording diffraction patterns from different sample parts at constant temperature. Especially suitable for this purpose are phase transitions with clear phase coexistence such as that shown in Fig. 8. By terminating heating scans within the coexistence region of the L_β-L_α transition in hydrated DPPE it was possible to maintain a stable ratio of the two coexisting phases for a long time. In case of narrow phase transitions such as the DPPE transition the variations of this ratio throughout the sample at constant temperature (positions a–d in Fig. 1 B) could be used as a rather sensitive indicator of stationary temperature gradients. The measurements with DPPE showed that these gradients did not exceed the fluctuation level in any particular sample portion from which diffraction data are recorded. The results for DPPE will be published subsequently (Yao, H., I. Hatta, R. D. Koynova, and B. G. Tenchov, manuscript in preparation).

Heating and cooling scans at 0.1°C/min through the main transition of DPPC are shown in Figs. 2 and 3, respectively. A most prominent feature of the transition in heating direction is a broadening of the diffraction lines in a narrow range of ~0.1°C at the transition midpoint. It is seen in Fig. 2 as a sharp drop of the peak intensity in the
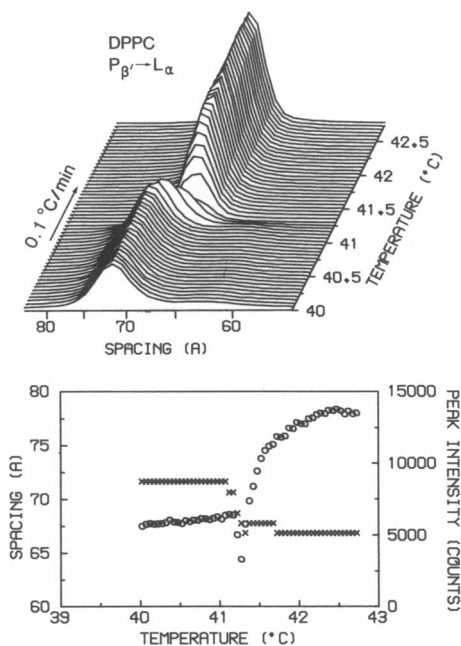
FIGURE 2 The main transition in fully hydrated DPPC (Avanti Polar Lipids, Inc.) multilayers recorded by low-angle x-ray diffraction at heating rate of 0.1°C/min. (×) Spacing; (○) peak intensity.
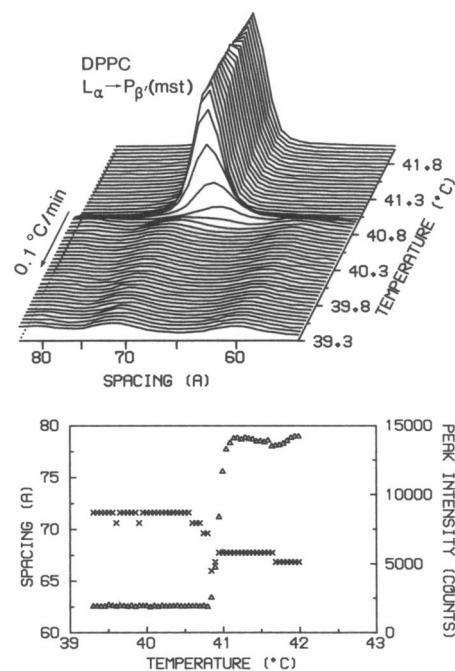

FIGURE 3 The main transition in fully hydrated DPPC (Avanti Polar Lipids, Inc.) multilayers recorded by low-angle x-ray diffraction in a cooling scan at 0.1°C/min. (×) Spacing; (△) peak intensity.

range 41.2–41.3°C. The minimum peak intensity coincides with the end of a shift of the lamellar spacing from its value in the rippled $P_{\beta'}$ phase (7.16 nm at 41°C) to the value typical of the liquid-crystalline L_{α} phase (6.69 nm at 42°C). This sequence of events was not fully reversible in cooling direction. Apart from a hysteresis of ~0.4°C, the initial diffraction pattern of the $P_{\beta'}$ phase was not recovered and a different profile appeared instead (Fig. 4). It consists of multiple peaks with low intensity. One of the peaks is identified with the original lamellar reflection in heating but the origin of the other peaks is not solved yet. Although the reflection due to the rippled structure was observed in heating as indicated by the arrow in Fig. 4, it was not found in cooling runs. These features were independent of cooling rates (0.05–0.5°C/min) and lipid sources (Sigma Chemical Co. and Avanti Polar Lipids, Inc.). The multiple-peak profile was stable for at least 30 min at a temperature in the rippled phase region. It was however readily converted into the initial $P_{\beta'}$ pattern by cooling to 25°C($L_{\beta'}$ phase region) and subsequent heating through the pretransition. Further in this paper we show by calorimetry that this pattern corresponds to a long-living metastable phase denoted as $P_{\beta'}$(mst).

Figs. 2 and 3 show that there is no coexistence between diffraction patterns of the gel and liquid-crystalline phases either in heating or in cooling direction. No evidence for such coexistence was found also in scans at 0.5 and 0.05°C/min (data not illustrated). Another note-

worthy common feature of the transitions in heating and cooling is that the spacing shifts occur at a slightly lower (by 0.10–0.15°C) temperature (Figs. 2 and 3) than the precipitate changes in the intensity of the lamellar reflections.

Heating scans through the subtransition and pretransition of DPPC are shown in Figs. 5 and 6, respectively. Typical of the subtransition is a monotonic change of the lamellar spacing from its subgel (L_{c}) value of 5.97 nm to the gel $L_{\beta'}$ value of 6.34 nm. The shape and width of the lamellar reflections were found to be constant during this transformation, as is evident also from Fig. 5. Although
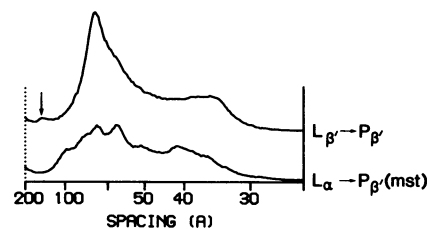

FIGURE 4 Diffraction profiles of the rippled phase of fully hydrated DPPC (Sigma Chemical Co.) recorded at 38.2°C after heating through the pretransition ($L_{\beta'}$-$P_{\beta'}$) at 0.5°C/min, and after cooling through the main transition (L_{α}-$P_{\beta'}$) at 0.5°C/min. Arrow indicates the first-order ripple reflection.
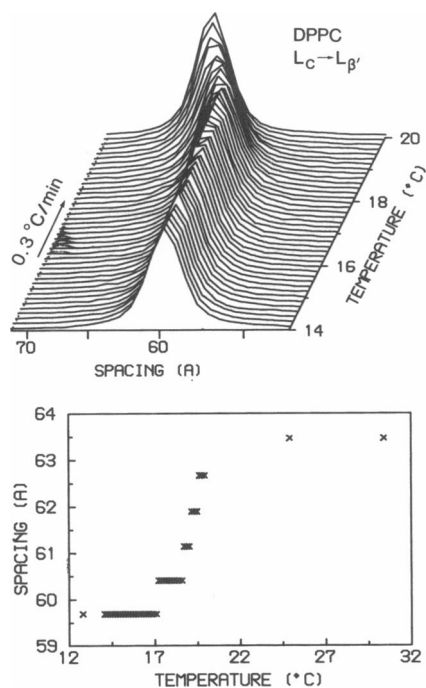
FIGURE 5 The subtransition in DPPC (Sigma Chemical Co.) after storage at 4°C for 50 d. The stepwise changes in the lamellar spacing are due to the discreteness of the PSPC (see Materials and Methods) whereas the actual change is smooth. The smooth line can be recovered easily by curve-fitting of sequential reflection shapes.

FIGURE 7 $L_{\beta'}$-L_α transition of DPPC (Avanti Polar Lipids, Inc.) in excess water containing 40 mg ethanol per ml water. (×) Spacing in heating; (○) peak intensity in heating; (△) peak intensity in cooling at 0.1°C/min.

illustrated in Fig. 6, the pretransition was not further investigated. Due to its slow kinetics, a comparison between transition mechanisms in heating and cooling would require a separate investigation.

With respect to the well-known biphasic effect of ethanol on the main transition of DPPC (18–20), measurements were made at low (40 mg ethanol per ml water) and high (80 mg/ml) ethanol concentrations (Figs. 7 and 8). At 40 mg/ml the lamellar periods of the gel and
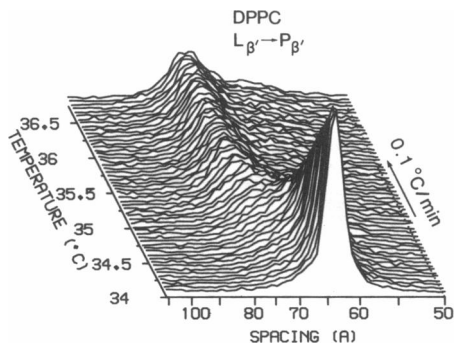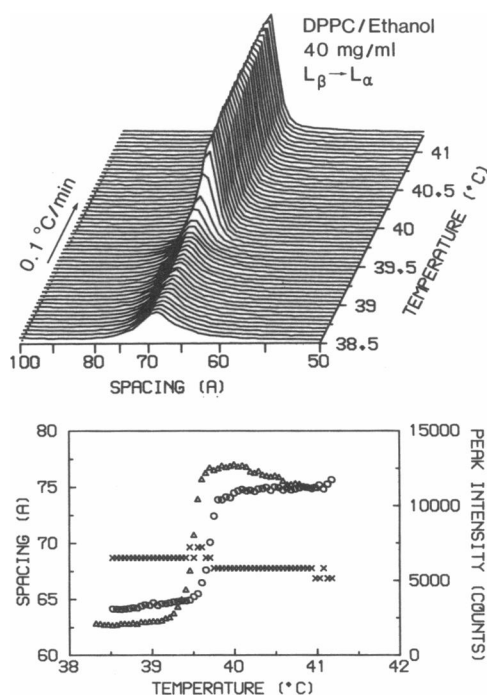
liquid-crystalline phases were almost identical (6.87 nm at 38.5°C and 6.69 nm at 41°C) and the only clear indication of the phase transition was a sharp increase of the peak intensity in the range 39.6–39.8°C (Fig. 7). The transition hysteresis of 0.2°C was two times smaller compared with DPPC in pure water. Ethanol concentration of 80 mg/ml induced formation of interdigitated gel phase (20) with a short lamellar period of 4.97 nm, whereas the lamellar period of the liquid-crystalline phase was unaffected (6.77 nm at 42°C). The phase transition between these two phases proceeds as a finite-range coexistence of the initial and final phases with no other structures detectable in the transition region. The coexistence regions in the diffraction patterns were 0.5°C in heating, and 0.8°C in cooling direction. The temperature hysteresis was ~1°C, much larger compared with DPPC in pure water (0.4°C) and at low ethanol concentration (0.2°C) at the same scan rate.

High-sensitivity DSC

Because the diffraction data suggest formation of two different $P_{\beta'}$ phases below the main transition of DPPC in pure water, one of them appearing after heating through the pretransition and the other one after cooling through

FIGURE 6 The pretransition in fully hydrated DPPC (Avanti Polar Lipids, Inc.) recorded at 0.1°C/min.
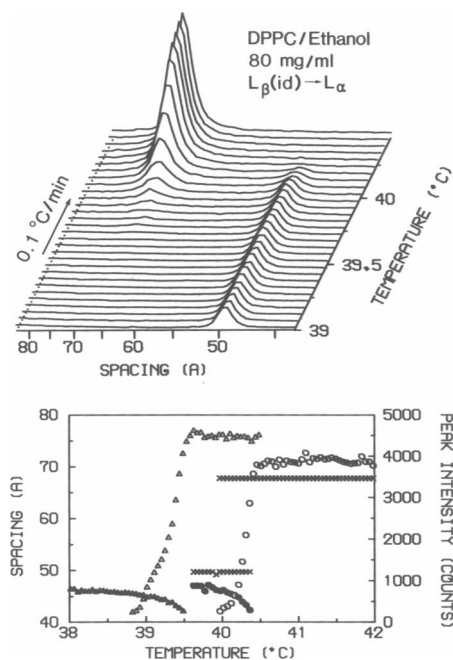
FIGURE 8 Interdigitated-gel/liquid-crystalline phase transition in fully hydrated DPPC (Avanti Polar Lipids, Inc.) containing 80 mg ethanol per ml water. (x) Spacing; (O) peak intensities in heating, (△) peak intensities in cooling at 0.1°C/min. Full and open symbols denote interdigitated and liquid-crystalline phases, respectively.

the main transition (Fig. 4), it is important to check for differences in the enthalpy of these two phases. The idea of the HSDSC measurements was to find out whether the enthalpy of the main transition depends on the particular low-temperature phase ($P_{\beta'}$ or $P_{\beta'}$[mst]) from which the lipid melting is accomplished. For this purpose, successive heating runs were made with the same sample but with different initial conditions. Each scan was preceded by cooling of the sample inside the calorimetric cell from 43°C to a temperature in the range 18–37°C and initiated immediately or after incubation at this temperature. A sequence of this type is presented in Table 1. Though the transition temperatures remain constant, both enthalpy and maximum excess specific heat C_p^{max} of the main transition are sensitive to the initial conditions and have lowest values in heating scans initiated at 37°C. It is evident also that the recovery of the pretransition strongly depends on the cooling prehistory and there is a correlation between the extent of this recovery and C_p^{max} of the main transition. The enthalpy of the main transition varies at most by 0.4 kcal/mol with temperature prehistory. However, the height appears to be more sensitive and its relative variations are much larger. We made no attempt to find eventual changes in the transition shape. Enthalpy variations of this magnitude are usually considered as within the error margin of such measurements. In

this case the reproducibility of the effect in repetitive scans and its consistency with a much better expressed variation of C_p^{max} allows us to conclude that the enthalpy of the main transition is lower by ~5% in heating scans initiated in the $P_{\beta'}$(mst) phase. It follows therefore that this phase has higher enthalpy and should be considered as metastable against the "standard" $P_{\beta'}$ phase which forms after heating through the pretransition.

It is important to note that this effect does not depend on the particular sequence of heating scans. Reshuffling of the sequence shown in Table 1 produces identical results.

AC calorimetry

The above described effect of cooling prehistory on the main transition of DPPC was very clearly expressed in AC calorimetric scans (Fig. 9 a). Though the transition temperature was constant, the peak height and the area in heating scans after 24 h incubation at 23°C, which was preceded by cooling from the liquid-crystalline phase, are more than three times as large as those at 38°C in the same thermal pretreatment. At present, we have no explanation for the much greater sensitivity of C_p (1 Hz) to the temperature prehistory as compared with the static excess C_p, but nevertheless, it is clear that the results of this experiment are fully consistent with both diffraction and HSDSC data concerning the existence of $P_{\beta'}$(mst) and show in addition that this is a relatively long-living phase. It does not convert into the "standard" $P_{\beta'}$ phase even after a 24-h incubation at 38°C but only by way of cooling to 23°C and subsequent reheating.

The DPPC main transition is almost irreversible in AC calorimetric scans (Fig. 9 b). The transition pathways in heating and cooling are quite different and the very low

TABLE 1 Effect of temperature prehistory on the main transition and pretransition in fully hydrated DPPC

Initial conditions	C_p^{max}	ΔH_{main}	ΔH_{pre}	T_{pre}
	kcal/K·mol	kcal/mol	kcal/mol	°C
Incubated for 4 h at 20°C	32.6	8.3	1.15	35.2
Initiated immediately at 20°C	31.8	8.2	1.04	34.9
Initiated immediately at 25°C	31.4	8.2	0.95	34.7
Incubated for 2 h at 25°C	32.2	8.3	0.97	35.0
Initiated immediately at 30°C	28.7	8.0	0.45	33.0
Incubated for 1 h at 30°C	30.3	8.1	0.86	34.2
Initiated immediately at 37°C	27.5	7.9	—	—
Incubated for 30 min at 37°C	27.5	7.9	—	—
Incubated overnight at 18°C	32.6	8.3	1.26	35.3

DPPC from Fluka AG. Transition characteristics were determined by HSDSC in successive heating scans with different initial conditions. The scan rate was 0.5°C/min and the scans were terminated at 43°C. The main transition temperature was constant in all scans. ΔH_{main} indicates the rounded values.
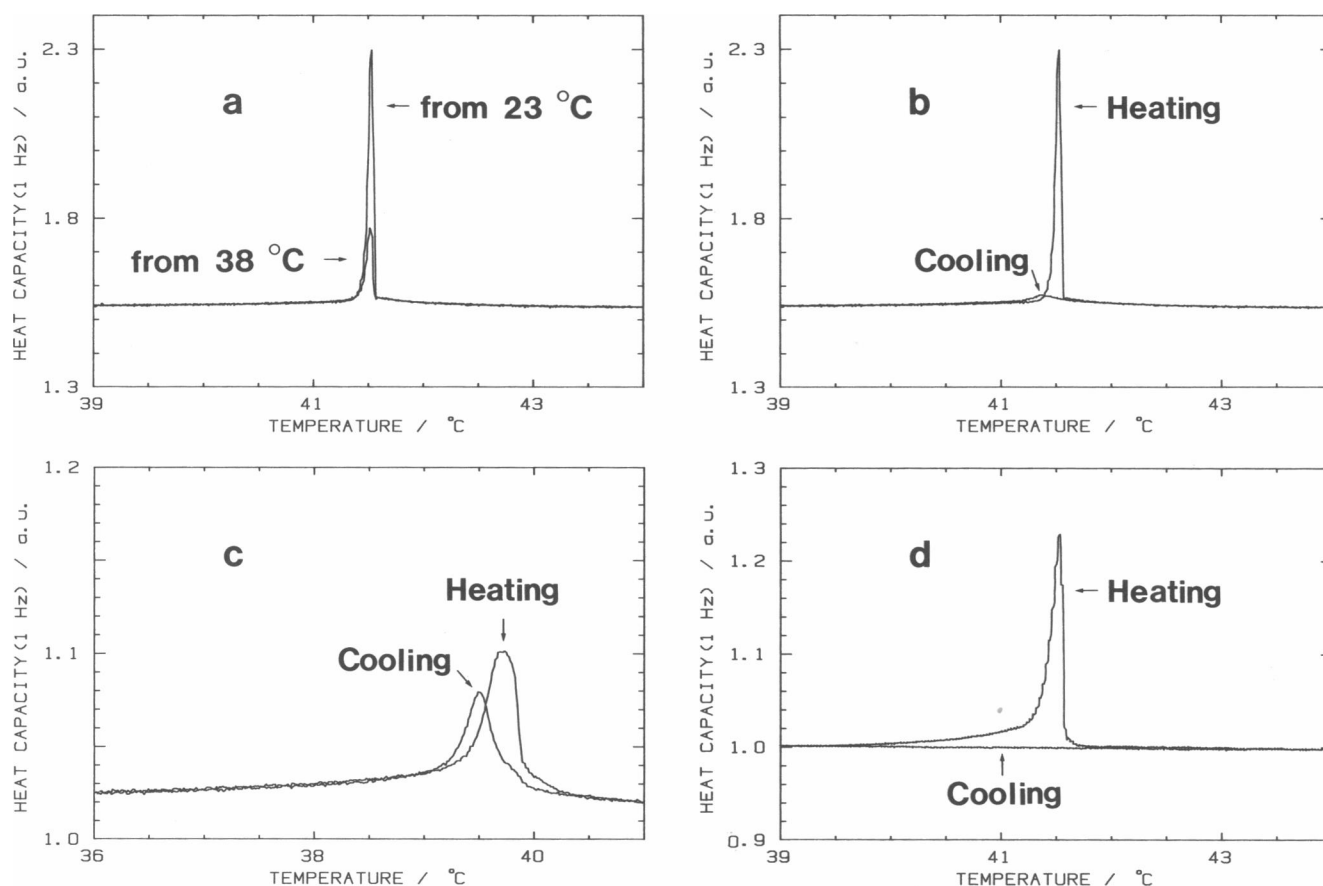
FIGURE 9 The main transition of DPPC (Avanti Polar Lipids, Inc.) in excess water and in DPPC/water/ethanol phases recorded by AC calorimetry. (a) DPPC in excess water; heating scans at 0.042°C/min from 23 and 38°C made after cooling from the liquid crystalline phase and incubation at these temperatures for 24 h; peak temperatures, 41.533 and 41.514°C, respectively; temperature oscillation, T_{ac} = 0.008°C. (b) DPPC in excess water; comparison of heating and cooling scans at 0.042°C/min; peak temperatures, 41.533 and 41.369°C; T_{ac} = 0.008°C. (c) Effect of 35 mg ethanol per ml water; scan rate 0.084°C/min; peak temperatures, 39.711 and 39.488°C; T_{ac} = 0.010°C. (d) Effect of 90 mg ethanol per ml water; scan rate 0.021°C/min; peak temperature, 41.537°C.

excess values of C_p (1 Hz) recorded in cooling direction indicate that the molecular rearrangements in the cooling transition have substantially longer response times to small heat stimuli. In an attempt to investigate further the transition irreversibility and to clarify the question which of the two pathways should be considered as closer to equilibrium, the time evolution of C_p(1 Hz) was followed at constant temperature between the peaks of the heating and cooling transitions, i.e., on the rising slope of the heating transition. An experiment of this type is shown in Fig. 10. There is no convergence between "heating" and "cooling" C_p (1 Hz) values >2 d. This proves the irreversibility of the DPPC main transition in AC calorimetry at low scan rates.

It was found however that ethanol has a profound (biphasic) effect especially on the "cooling" C_p(1 Hz) values. At low ethanol concentration the phase transition became almost reversible (Fig. 9 c), whereas at high

ethanol concentration the C_p(1 Hz) anomaly in cooling direction completely disappeared (Fig. 9 d).

DISCUSSION

"Large-scale" and "small-scale" coexistence

Because the discussion deals with lipid phase coexistence in relation to its observability by x-ray diffraction, it is convenient to introduce two terms. By "large-scale" coexistence we denote coexistence of large enough three-dimensional domains of the two phases which give coexisting reflections in the diffraction pattern; these reflections are identical to those from each single phase (see, e.g., Fig. 8). If stable, a "large-scale" coexistence is also a phase coexistence from thermodynamic viewpoint. Alternatively, a "small-scale" coexistence denotes coexistence
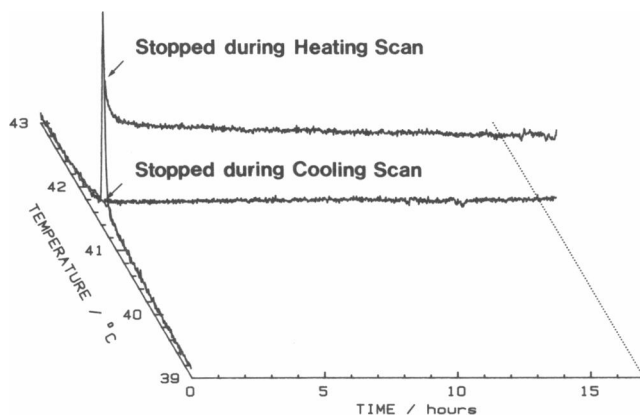
FIGURE 10 Time dependence of "heating" and "cooling" excess values of the dynamic heat capacity C_p (1 Hz) recorded by AC calorimetry at temperatures 41.306 ± 0.005 and 41.313 ± 0.005°C reached by heating and cooling, respectively, at scan rate 0.042°C/min. T_{ac} = (1.22 – 1.35) × 10^{-3}°C.

of uncorrelated two-dimensional domains or small three-dimensional domains which do not give coexisting single-phase patterns and may or may not be phases in thermodynamic sense. The diffraction profile in this case cannot be predicted but it might be expected that it will consist of broadened reflections due to disrupted correlations and inhomogeneous lamellar spacing. We cannot set a boundary between these two types of coexistence in terms of domain size but suspect that it is a few tens of lamellar periods.

A "small-scale" coexistence applies also to coexistence of a large phase with small domains of the other phase. In this case the diffraction pattern will be dominated by that of the large phase.

Lack of "large-scale" coexistence in the main transition of DPPC

As clear from the description of the diffraction data, a characteristic feature of the main transition at low scan rate is a lack of "large-scale" coexistence between the gel and liquid-crystalline phases. This is obvious from Fig. 2, where a narrow intensity gap caused by broadening of the lamellar reflections serves as a demarcation line between the two phases. This broadening most probably reflects a disorder in bilayer stacking and a partial loss of correlation in the lamellar structure during chain melting. It is well expressed in two successive frames of 1 min total duration. The disordered state may not be a true equilibrium state over the whole temperature range of 0.1°C, where it is observed but it is still evident that a slow rearrangement in bilayer stacking mediates the transition from the rippled to the liquid-crystalline phase and sepa-

rates the two phases on the temperature scale. The intermediate disordered state is consistent with a "small-scale" coexistence. Such lamellar disorder should be expected as a result of the appearance of multiple small liquid domains in the solid phase. Their growth leads to disruption of the gel phase and formation of the liquid-crystalline phase in a way avoiding "large-scale" coexistence in the transition region. This picture is representative for a volume of ∼1 mm³ from which diffraction data are collected.

In this connection it is pertinent to recall previous studies by low-angle time-resolved (2, 4, 6) and static x-ray diffraction (26), which report a finite-range "large-scale" phase coexistence in the main transition of DPPC, in apparent contradiction to our results. Gottlieb and Eanes (26) and Caffrey and Bilderback (2) have observed stable "large-scale" coexistence in a definitely finite temperature range by measurements at constant temperatures and in conditions excluding the possibility that this effect might be due to temperature gradients or instabilities within the samples. An examination of sample descriptions and values of lamellar spacings shows, however, that these measurements have been carried out at water contents below the level of excess water (5–24 wt% in reference 26 and ∼20 wt% in reference 2, whereas for the liquid-crystalline phase of DPPC this level is ∼36 wt% in reference 15). This is obvious also from the lamellar spacings recorded for the liquid-crystalline phase (5.81 nm at 24 wt% of water [26] and 4.7 nm [2]) which are much shorter than the lamellar spacing of 6.7 nm for the L_α phase of DPPC in excess water (see, e.g., reference 13 and Figs. 2 and 3). Below the level of excess water the phase diagram of the DPPC/water system is determined by the ratio of the two components. It is well known that in such binary phase diagrams the solidus and liquidus lines are separated in temperature and encircle a finite range of stable coexistence of the solid and liquid phases. Considering this, we believe that the finite-range "large-scale" coexistence in the melting transition of DPPC found in references 2 and 26 amounts to a manifestation of the properties of the binary phase diagrams. These results by no means contradict the conclusion that there is no such coexistence in presence of excess water where the phase behavior of DPPC does not depend on the water concentration and the hydrated multilayers can be considered as one-component system from a phase rule viewpoint. This argument shows also that there is no reason to consider these results as contradicting the Gibbs phase rule. The discussion on a possible violation of this rule in lipid-water systems (26), although of certain interest with respect to such systems, appears to be irrelevant to the particular DPPC/water system investigated in this work.

In kinetic studies on lipid phase transitions, Laggner et

al. (4, 6) have observed a "large-scale" coexistence in the main transition of DPPC in excess water over a broad temperature range of ~3°C. Because these measurements have been made during temperature jumps at 1–2°C/s, they characterize the transition mechanism and kinetics along a nonequilibrium pathway and cannot be directly compared or considered as inconsistent with the present measurements which have been made in conditions much closer to equilibrium (~1,000 times lower scan rate and absence of temperature gradients).

Summarizing the discussion up to here, we conclude that there are no actual contradictions between previous and present results with respect to the mechanism of the main transition in DPPC. A finite-range "large-scale" phase coexistence appears at low water contents and also during temperature jumps but there is no such coexistence under conditions of excess water and of slow uniform temperature scans. This picture is consistent with the phase rule and provides no reason to doubt its applicability, at least to DPPC/water phases.

Irreversibility of the main transition

The diffraction, HSDSC and AC calorimetry data recorded in this work consistently show that the main transition of DPPC is not reversible in the sense that the initial $P_{\beta'}$ phase does not reappear even on very slow cooling from the L_α phase, but is replaced by a different phase $P_{\beta'}(mst)$. The latter phase is long living at constant temperature in the rippled phase region but can be readily converted back to the initial $P_{\beta'}$ by cooling to the $L_{\beta'}$ region and reheating subsequently through the pretransition. This behavior is summarized in Fig. 11. Strictly speaking, the $P_{\beta'}(mst)$ may not be a truly metastable phase but just an unstable state with very long relaxation time (slow relaxations in the rippled phase of phosphatidylcholines are a well-known phenomenon [6, 27,28]). This ambiguity cannot be readily resolved and we denote the phase as metastable on the grounds that the data reported here provide no evidence for the existence of a relaxation process. Its higher enthalpy compared with the $P_{\beta'}$ phase was made apparent by HSDSC (Table 1) and especially by AC calorimetry (Fig. 9 a). Actually, it is surprising that the simple effect of temperature prehistory on the main transition of DPPC has not been noticed earlier in the numerous DSC studies on this system. The small enthalpy difference of ~5% between the $P_{\beta'}-L_\alpha$ and $P_{\beta'}(mst)-L_\alpha$ phase transitions and the difference in diffraction patterns suggests that $P_{\beta'}(mst)$ should not be considered as less solid than $P_{\beta'}$ but rather as less ordered with respect to correlations and stacking of the bilayers. It is conceivable that after a disordered state has been fixed in the cooling main transition, an ordering process resulting in better correlated rippled bilayers might be strongly
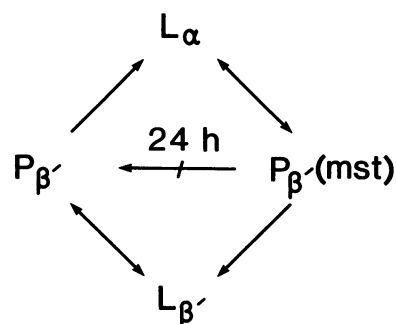

FIGURE 11 Scheme of heating and cooling phase sequences in fully hydrated DPPC involving a stable $P_{\beta'}$ phase and a long-living metastable state $P_{\beta'}$ (mst).

hindered and require a very long time, especially as it is driven by a small thermodynamic force. In such appearances of $P_{\beta'}(mst)$, the question of whether this is a metastable or a long-living unstable state is not of significant physical interest. A screening of the experimental procedures used in x-ray diffraction studies of the rippled phase structure afforded no direct clues whether the phase had actually been studied in heating or cooling, but it seems that the well-aligned rippled phase has been formed by heating through the pretransition (12, 13).

The very interesting dynamic aspects of the main transition irreversibility revealed by AC calorimetry (Figs. 9 and 10) cannot be understood at present in detail for the absence of a concept ascribing the excess values of the dynamic heat capacity to specific molecular rearrangements during the transition. In spite of this, there are at least two conclusions requiring attention and further investigation. First, the transition pathways in heating and cooling are distinctly different and do not converge at constant temperature (Fig. 10). Second, the lipid bilayer response times at the main transition in cooling are substantially longer (Fig. 9 b). Similar to that shown in Fig. 9 b the irreversibility of the main transition has been observed by AC calorimetry also at a lower oscillation frequency of 0.03 Hz (29).

Ethanol effects

Comparison of Figs. 2, 7, 8, and 9 b–d, corroborates all of the principal conclusions reached in previous work (18–20). Besides a biphasic effect on the main transition temperature (18, 19), these include transition reversibility at low ethanol concentrations, as opposed to irreversibility at high concentrations (19), and formation of interdigitated gel phase at high ethanol concentrations (20). The formation of this phase provides the basis for interpretation of the biphasic ethanol effect (20). The present data show also that ethanol strongly affects the

transition mechanism. Fig. 7 shows a rather unusual example of phase transition that is not accompanied by change of the lamellar period. In this transition the decrease of bilayer thickness caused by chain melting appears to be precisely compensated by increase of water layer thickness. Because such compensation eliminates the necessity for contraction or expansion of the total thickness of the lipid multilayers, it might influence the transition kinetics and serve as a possible explanation of the transition reversibility observed by Rowe (19) and considerably smaller hysteresis loop compared with DPPC in pure water and at high ethanol concentration (Figs. 2, 3, 7, 8). Due to the identical lamellar periods of the gel and liquid-crystalline phases, the diffraction data in Fig. 7 provides no evidence concerning the type of phase coexistence in this transition. However, a "large-scale" coexistence was clearly expressed between the interdigitated gel and liquid-crystalline phases (Fig. 8). Because no measurements were made at constant temperature, at present it remains unclear to what extent the finite temperature range of this coexistence is determined by the transition kinetics.

DPPC subtransition

With account of scan rate (0.3°C/min) and storage time at 4°C (50 d), the temperature of the subtransition shown in Fig. 5 agrees well with the scan rate dependence reported for this transition by Tristram-Nagle et al. (30). It proceeds as a smooth shift of the lamellar spacing from its subgel to its gel value over a temperature range of 3 to ~4°C compatible with the transition width recorded by HSDSC under similar conditions (30). The lack of broadening in the intermediate lamellar reflections is indicative of the subtransition mechanism. First, the process is homogeneous over the whole macroscopic volume of ~1 mm³ from which diffraction is recorded. Second, it seems to deny any simple picture for coexistence of the subgel and gel phases in the transition region. A "large-scale" coexistence is excluded as it would result in two separate lamellar reflections (see examples of such coexistence in Fig. 8 and also in our upcoming paper [Yao, H., I. Hatta, R. D. Koynova, and B. G. Tenchov, manuscript in preparation] for the phase transitions in DPPE). The remaining possibility for a "small-scale" coexistence is more difficult to assess because various realizations of such coexistence are conceivable. Still, by analogy with the main transition of DPPC (Fig. 2), it seems reasonable to expect that in most cases a "small-scale" coexistence will be accompanied by perceptible broadening of the intermediate lamellar reflections. Thus, the diffraction data cannot be reconciled in a straightforward way with models assuming growth of domains of the final phase within the initial phase. A model of this type has been considered

in ref. 31. A picture of the subtransition within the framework of such models must satisfy at least three conditions: (a) only "small-scale" coexistence is permissible; (b) the "small-scale" coexistence must not broaden the diffraction lines; (c) it must ensure a smooth shift of the lamellar spacing between its subgel and gel values.

Fig. 5 shows the result obtained in nonequilibrium (scan rate 0.3°C/min), whereas a sharper transition occurs at 13.8°C in equilibrium (17, 30). If "large scale" phase coexistence takes place in a certain system in nonequilibrium, there can be two cases in equilibrium: one is the case without "large-scale" coexistence as shown in Fig. 2 for the main transition of DPPC and the other is the case with such coexistence as genuine feature of the system. On the other hand, if a "large-scale" coexistence does not take place in nonequilibrium (Fig. 5), no such coexistence can be expected also in equilibrium. Furthermore, static x-ray diffraction studies on the formation of the DPPC subgel phase (32, 33) show a reversal of the process in Fig. 5 except for a much longer time scale, i.e., the formation of the subgel phase upon incubation at 1.5°C is accompanied by a smooth shift of the lamellar reflection from its gel to its subgel value with no broadening in the intermediate positions. In addition, the wide-angle diffraction pattern also appears to change continuously (16, 33). Its evolution proceeds via splitting of the initial $L_{\beta'}$ peak at 0.42 nm and slow monotonic shifts of the two peaks until their positions are reached to the ultimate ones in the subgel phase. Although at a very high scan rate of 5°C/min, a reversal of the continuous changes at wide angles has been observed in heating through the subtransition (8). In sum, all of the diffraction data show that the above three conditions must be satisfied by a theoretical model for both directions of the subgel-gel transformation. These conditions appear to be incompatible with growth of three-dimensional domains of one phase within the other phase. It might be possible to construct a mosaic of growing two-dimensional domains satisfying at least the requirements of the low-angle diffraction, but the actual transition mechanism might be more complex. In fact, the analysis of the transition kinetics by Yang and Nagle (31) has unveiled unusually low (close to unity) effective dimensionality of the growing domains and has encountered difficulties in relating this low value to domain growth of higher dimension.

Because the type of decay law by itself does not uniquely determine the microscopic relaxation mechanism responsible for its appearance, it is useful to consider alternative mechanisms. Here we propose an alternative mechanism based on "sequential" relaxation of the lipid phases. A sequential relaxation might occur if the time required for formation of macroscopic cooperative units in the intermediate transition states is shorter than the

relaxation time between the initial and final phases. In this case the transition will be represented by a continuous, space-uniform transformation of one phase into the other. At no point in this process do the initial and final phases coexist.

The sequential relaxation mechanism is consistent with the diffraction data. Because it is unidirectional, it can explain (but in different terms) also the close-to-unity effective dimensionality of the growing domains. However, the plausibility of the underlying assumption and, consequently, the applicability of a sequential relaxation scheme to the subgel-gel transformations remains unclear and requires additional analysis.

REFERENCES

1. Ranck, J. L., L. Lettellier, E. Schechter, B. Krop, P. Pernod, and A. Tardieu. 1984. X-Ray analysis of the kinetics of *Escherichia coli* lipid and membrane structural transitions. *Biochemistry*. 23:4955–4961.

2. Caffrey, M., and D. Bilderback. 1984. Kinetics of the main phase transition of hydrated lecithin monitored by real time x-ray diffraction. *Biophys. J.* 45:627–631.

3. Caffrey, M. 1985. Kinetics and mechanism of the lamellar gel/lamellar liquid-crystal and lamellar/inverted hexagonal phase transition in phosphatidylethanolamine: a real-time x-ray diffraction study using synchrotron radiation. *Biochemistry*. 24:4826–4844.

4. Laggner, P. 1988. X-Ray studies on biological membranes using synchrotron radiation. *Top. Curr. Chem.* 145:175–202.

5. Laggner, P. 1986. Structural Biological Uses of X-Ray Absorption, Scattering and Diffraction. B. Chance and H. D. Bartunik, editors. Academic Press, Inc., New York. 171–182.

6. Laggner, P., K. Lohner, and K. Müller. 1987. X-Ray cinematography of phospholipid phase transformations with synchrotron radiation. *Mol. Cryst. Liq. Cryst.* 151:373–388.

7. Tamura-Lis, W., L. J. Lis, and P. J. Quinn. 1987. Structures and mechanisms of liquid phase transitions in nonaqueous media: dipalmitoylphosphatidylcholine in fused salt. *J. Phys. Chem.* 91:4625–4627.

8. Tenchov, B. G., L. J. Lis, and P. J. Quinn. 1987. Mechanism and kinetics of the subtransition in hydrated L-dipalmitoylphosphatidylcholine. *Biochim. Biophys. Acta*. 897:142–151.

9. Koynova, R. D., B. G. Tenchov, P. J. Quinn, and P. Laggner. 1988. Structure and phase behavior of hydrated mixtures of L-dipalmitoylphosphatidylcholine and palmitic acid. Correlations between structural rearrangements, specific volume changes and endothermic events. *Chem. Phys. Lipids*. 48:205–214.

10. Ladbrooke, B. D., and D. Chapman. 1968. Thermal analysis of lipids, proteins and biological membranes. A review and summary of some recent studies. *Chem. Phys. Lipids*. 3:304–367.

11. Tardieu, A., V. Luzzati, and F. C. Reman. 1973. Structure and polymorphism of the hydrated chains of lipids: a study of lecithin-water phases. *J. Mol. Biol.* 75:711–733.

12. Janiak, M. J., D. M. Small, and G. G. Shipley. 1976. Nature of the thermal pretransition of synthetic phospholipids: dimyristoyl- and dipalmitoyllecithin. *Biochemistry*. 15:4575–4580.

13. Inoko, Y., and T. Mitsui. 1978. Structural parameters of dipalmitoylphosphatidylcholine lamellar phases and bilayer phase transitions. *J. Phys. Soc. Jpn*. 44:1918–1924.

14. Albon, N., and J. M. Sturtevant. 1978. Nature of the gel to liquid crystal transition of synthetic phosphatidylcholines. *Proc. Natl. Acad. Sci. USA*. 75:2258–2260.

15. Chen, S. C., J. M. Sturtevant, and B. J. Gaffney. 1980. Scanning calorimetric evidence for sub-phase transition in phosphatidylcholine bilayers. *Proc. Natl. Acad. Sci. USA*. 77:5060–5063.

16. Fuldner, H. H. 1981. Characterization of a third phase transition in multilamellar dipalmitoyllecithin liposomes. *Biochemistry*. 20:5707–5710.

17. Nagle, J. F., and D. A. Wilkinson. 1982. Dilatometric studies of the subtransition in dipalmitoylphosphatidylcholine. *Biochemistry*. 21:3817–3821.

18. Rowe, E. S. 1983. Lipid chain length and temperature dependence of ethanol-phosphatidylcholine interactions. *Biochemistry*. 22:3299–3305.

19. Rowe, E. S. 1985. Thermodynamic reversibility of phase transitions. Specific effects of alcohols on phosphatidylcholines. *Biochim. Biophys. Acta*. 813:321–330.

20. Simon, S. A., and T. J. McIntosh. 1984. Interdigitated hydrocarbon chain packing causes the biphasic transition behavior in lipid/alcohol suspensions. *Biochim. Biophys. Acta*. 773:169–172.

21. Amemiya, Y., K. Wakabayashi, T. Hamanaka, T. Wakabayashi, T. Matsushita, and H. Hashizume. 1983. Design of a small-angle x-ray diffractometer using synchrotron radiation at the Photon Factory. *Nucl. Instrum. Methods*. 208:471–477.

22. Privalov, P. L. 1980. Scanning microcalorimeters for studying macromolecules. *Pure Appl. Chem.* 52:479–497.

23. Hatta, I., and A. J. Ikushima. 1981. Studies on phase transitions by AC calorimetry. *Jpn. J. Appl. Phys.* 20:1995–2011.

24. Yao, H., and I. Hatta. 1988. An ac microcalorimetric method for precise heat capacity measurement in a small amount of liquid. *Jpn. J. Appl. Phys.* 27:L121–L122.

25. Caffrey, M. 1985. X-Radiation damage of hydrated lecithin membranes detected by real-time x-ray diffraction using wiggler-enhanced synchrotron radiation as the ionizing radiation source. *Nucl. Instrum. Methods*. 222:329–338.

26. Gottlieb, M., and E. Eanes. 1974. Coexistence of rigid crystalline and liquid-crystalline phases in lecithin-water mixtures. *Biophys. J.* 14:335–342.

27. Lentz, B. R., Y. Barenholz, and T. E. Thompson. 1976. Fluorescence depolarization studies of phase transition and fluidity in phospholipid bilayers. 1. Single component phosphatidylcholine liposomes. *Biochemistry*. 15:4521–4528.

28. Akiyama, M., S. Matuoka, S. Kato, I. Hatta, Y. Amemiya, and Y. Terayama. 1987. Slow change of $P_{\beta'}$ structure after temperature jump across main transition in dimyristoylphosphatidylcholine. *In* Photon Factory Activity Report. National Laboratory for High Energy Physics. Tsukuba, Japan. 342.

29. Imaizumi, S., and C. W. Garland. 1987. AC calorimetric studies on main transition in dipalmitoylphosphatidylcholine (DPPC). *J. Phys. Soc. Jpn.* 56: 3887–3892.

30. Tristram-Nagle, S., M. Wiener, C. P. Yang, and J. F. Nagle. 1987. Kinetics of the subtransition in dipalmitoylphosphatidylcholine. *Biochemistry.* 26:4288–4294.

31. Yang, C. P., and J. F. Nagle. 1988. Phase transformations in lipids follow classical kinetics with small fractional dimensionalities. *Phys. Rev. A.* 37:3993–4000.

32. Akiyama, M. 1985. X-Ray diffraction study of subtransition in dipalmitoylphosphatidylcholine. *Jpn. J. Appl. Phys.* 24:231–234.

33. Akiyama, M., N. Matsushima, and Y. Terayama. 1987. Kinetics of the subtransition of multilamellar dipalmitoylphospatidylcholine. *Jpn. J. Appl. Phys.* 26:1587–1591.